



Optimal Access Point Selection Approach for User-Centric Cell-Free Massive MIMO Systems

Weifeng Ma¹, Xinghua Sun^{1(✉)}, Xijun Wang², and Wen Zhan¹

¹ School of Electronics and Communication Engineering, Sun Yat-sen University,
Shenzhen 518107, China

mawf3@mail2.sysu.edu.cn, {sunxinghua,zhanw6}@mail.sysu.edu.cn

² School of Electronics and Information Technology, Sun Yat-sen University,
Guangzhou 510006, China

wangxijun@mail.sysu.edu.cn

Abstract. Recently, the Cell-Free Massive Multiple-Input Multiple-Output (MIMO) architecture has emerged as a promising solution for future wireless communication systems, where a substantial number of distributed wireless Access Points (APs) concurrently serve a significantly smaller count of User Equipment (UE). In this paper, we study the AP selection problem in user-centric cell-free massive MIMO, where each user is served by a restricted number of APs. To address this problem, we propose a Branch-And-Bound (BAB)-based AP selection algorithm to achieve maximum channel capacity, which is designed to efficiently obtain the optimal subset of APs for each user. Our simulation results show that the proposed algorithm outperforms other baseline methods in terms of channel capacity at the expense of some complexity. Meanwhile, our complexity is much lower than the exhaustive search, which also yields optimal results.

Keywords: Cell-Free Massive MIMO · User-Centric · AP selection

1 Introduction

Cell-Free Massive Multiple-Input Multiple-Output (MIMO) has emerged as a promising alternative network topology, attracting considerable interest due to its potential to mitigate inter-cell interference under the conventional cellular structure [1]. In cell-free massive MIMO networks, a multitude of geographically dispersed wireless Access Points (APs) are linked to a Central Processing Unit (CPU) through optical fibers, cooperatively serving all users by conjugate beamforming [2]. However, under this architecture, every user is simultaneously served by all available APs, leading to an elevated workload for each AP and a substantial increase in backhaul overhead [3]. To facilitate practical implementation [4], a user-centric framework is gaining increasing momentum, wherein each user is served exclusively by a restricted number of APs [5].

In a User-Centric Cell-Free Massive MIMO system, every user is surrounded by neighboring serving APs, thereby forming a virtual cell [6]. This provides the following benefits: initially, each AP serves a subset of users, efficiently reducing the burden and power consumption. Furthermore, the data transmission from the AP to the CPU is minimized, resulting in a significant reduction in backhaul overhead. A proper AP selection scheme then becomes crucial since otherwise users can not obtain a good Quality of Service (QoS) [5] or high energy efficiency [7].

Several studies have been performed to obtain user-centric virtual cells by AP selection in cell-free massive MIMO networks [8–15]. One approach involves the user selecting a predetermined number of APs based on the optimal channel quality or minimal distance criteria [8–11]. Alternatively, each user can select the APs that collectively contribute a specified percentage to the overall channel gain [12, 13]. In addition, the work [14] proposed a method named Average Channel Gain Based (ACGB) selection, i.e., each AP computes the average specification of the estimated channels of all User Equipment (UE), subsequently serving those UE whose channel specification is greater than the average. The work [15] investigated the problem from a game-theoretic perspective and formulated the creation of user-centric AP service clusters as a localized altruistic game. However, none of the above schemes can reach the upper limit of channel capacity for an individual user.

In this paper, we address the problem of selecting an appropriate subset of APs in the context of user-centric cell-free massive MIMO. Specifically, we derive the channel capacity in this scenario as our objective, followed by constructing a new objective function. This function applies to the Branch-And-Bound [16] (BAB) algorithm, which is commonly used to solve integer programming problems. Finally, a BAB-based AP selection algorithm is proposed to efficiently obtain an optimal solution to maximize the channel capacity. By comparing our approach with other baseline approaches, we find that the proposed method achieves better performance with an acceptable increase in computational complexity. To the best of our knowledge, this is the first research on AP selection schemes for individual users in cell-free massive MIMO systems, aiming at channel capacity optimization.

The remainder of the paper is structured as follows. In Sect. 2, we present the channel model of cell-free massive MIMO and derives the channel capacity expression. Section 3 describes the principle and detailed implementation of the BAB-based AP selection algorithm. Numerical results and discussions are provided in Sect. 4. Finally, we conclude the paper in Sect. 5.

2 System Model

Consider a user-centric cell-free massive MIMO network containing one UE and N access points. Within this cell-free network, a total of N geographically dispersed APs are all interconnected to a CPU through optical fibers, collectively providing service to the UEs. As Fig. 1 illustrates, each AP equips one single

antenna and scatters randomly around the UE, whereas the UE is equipped with $M \geq 1$ antennas. We assume a flat fading channel, and it is presumed that the channel state information from all APs to the UE is accessible. Note that the analysis within this work focuses on the downlink scenario, the analysis can be extended to the uplink scenario due to the channel's symmetry.

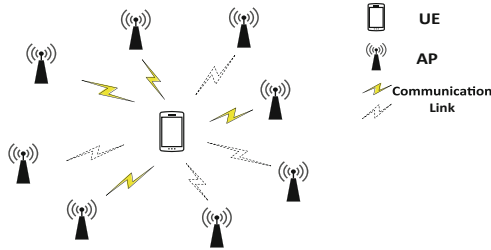


Fig. 1. A graphical illustration of the user-centric cell-free massive MIMO scenario containing one UE and N randomly-located APs, where the antennas at the UE are omitted for simplicity.

2.1 Channel Model

In the proposed network, the received signal at the UE through the channel fading, denoted as \mathbf{r} , is given by

$$\mathbf{r} = \mathbf{H}\mathbf{s} + \mathbf{n}, \quad (1)$$

where \mathbf{s} denotes the $(N \times 1)$ transmitted signal. Here, \mathbf{n} represents additive Gaussian noise with a zero mean and a variance of σ_n^2 . Specifically, \mathbf{H} represents an $M \times N$ channel matrix, within which each h_{mk} signifies the fading coefficient between the m th antenna at the user and the k th access point, where $m \in \{1, 2, \dots, M\}$ and $k \in \{1, 2, \dots, N\}$. These coefficients are related to the distance vector $d = [d_1, d_2, \dots, d_N]^T$, where d_k signifies the distance between the user and the k th AP. Hence, the channel matrix \mathbf{H} can be written as

$$\mathbf{H} = [\mathbf{h}_1(d_1), \mathbf{h}_2(d_2), \dots, \mathbf{h}_N(d_N)], \quad (2)$$

where $\mathbf{h}_k(d_k) = [h_{1k}(d_k), h_{2k}(d_k), \dots, h_{Mk}(d_k)]^T$.

Moreover, this study has taken into account a comprehensive compound channel model that encompasses the cumulative impact of path loss, shadow fading, and small-scale fading. The path loss is determined according to the fading with an exponent denoted by α , while the shadow fading is modeled using a normal distribution. Additionally, the small-scale fading follows a Rayleigh fading distribution. Let $s_k(d_k)$ refers to the average mean power of the shadow fading, then its logarithmic form s_{dB} satisfies the following distribution

$$s_{dB} = 10 \lg(s_k(d_k)) \sim \mathcal{N}(u_{dB}, \sigma_{dB}^2), \quad (3)$$

where σ_{dB} is the standard variance of $10\lg(s_k(d_k))$, μ_{dB} represents the logarithmic mean of $s_k(d_k)$ measured in dB, and $\mathcal{N}(\mu_{dB}, \sigma_{dB}^2)$ denotes Gaussian distribution with mean μ_{dB} and variance σ_{dB}^2 . Furthermore, u_{dB} is determined by the path loss and can be obtained from

$$u_{dB} = 10\lg(P_T/N) - \alpha \times 10 \times \lg(d_i), \quad (4)$$

where P_T represents the total transmitted power from all the N APs and α represents the exponent of path loss.

Combining Eqs. (3) and (4), the fading coefficient between the m th antenna at the user and the k th access point with a distance d_k , denoted as $h_{mk}(d_k)$, can be obtained as

$$h_{mk}(d_k) = \mathcal{N}(0, \sqrt{\frac{s_k(d_k)}{2}}) + j\mathcal{N}(0, \sqrt{\frac{s_k(d_k)}{2}}). \quad (5)$$

2.2 Channel Capacity

In this paper, we assume perfect Channel State Information (CSI) is available at the transmitter, and the channel is considered to be independent and identically distributed (i.i.d). Supposing that the total transmitted power is set at a unit magnitude and the water-filling power allocation is applied, which is confirmed to be optimal. The transmission power of the k th AP when applying the water-filling method, denoted as P_k is given by

$$P_k = \max\left(\left(u - \frac{\sigma^2}{\|\mathbf{h}_k\|^2}\right), 0\right), \quad (6)$$

where \mathbf{h}_k is the k th column of \mathbf{H} , $k \in \{1, 2, \dots, N\}$. Here u is a global constant and should be properly chosen to guarantee

$$P_{total} = \sum_{k=1}^N P_k = 1. \quad (7)$$

Referring to the channel analysis of distributed MIMO in [17] and combining Eqs. (6) and (7), we can derive the channel capacity of the MIMO system C as follows:

$$C = \log_2 \det[\mathbf{I}_M + \frac{1}{\sigma_n^2} \mathbf{H} \mathbf{Q} \mathbf{H}^H], \quad (8)$$

where $\mathbf{Q} = \text{diag}(P_1, P_2, \dots, P_N)$ represents the power allocation matrix at the transmitter, subject to the constraint $\text{tr}(\mathbf{Q}) = P_T$, and \mathbf{I}_M is an M -dimensional identity matrix, while σ_n^2 corresponds to the variance of additive Gaussian noise and the operator $(\cdot)^H$ denotes conjugate transpose.

3 Bab-Based Selection Algorithm

In the previous sections, we have characterized the channel matrix \mathbf{H} as well as the channel capacity C in the proposed user-centric cell-free massive MIMO scenario. Intuitively, as the number of available APs arises, better communication service quality guarantees to the UE. To optimize energy utilization and conserve total transmit power, a fixed number of APs are selected and connected to the UE. Hence, in this section, we focus on the optimization of the channel capacity C considering the constraint that the maximum amount of the optional APs, denoted as L and $0 < L \leq N$, for the UE to access each time is restricted.

The above AP selection problem could be further formulated as a mathematical matrix subset selection problem, which exhibits striking similarities to the problems of antenna selection and beam selection and numerous algorithms have been employed to address this type of problem. Among all the existing algorithms, the Branch-And-Bound (BAB) algorithm exhibits significant potential in attaining the global optimal solution while reducing complexity, compared with the exhaustive search [18]. The fundamental concept of the BAB algorithm revolves around constructing a search tree while incorporating pruning operations.

Specifically, the objective of the AP selection problem addressed in this paper is to derive the optimal L -amount subset out of N available APs considering the channel condition from each AP, in order to obtain the maximum channel capacity in the restricted situation. To tackle this problem, the BAB algorithm will be applied as the proposed solution methodology.

Note that performing a water-filling algorithm for each potential selection outcome can impose a significant computational burden. Hence we simplify the problem by initially assuming an average power distribution during the AP selection process and employing the water-filling method on the selected result to obtain the optimal power allocation scheme.

Let \mathbf{H}_{opt} denotes the optimal channel matrix after selecting the optimal L -amount AP subset in the proposed network, which could be derived as

$$\mathbf{H}_{opt} = \arg \max_{\mathbf{H}_{sub} \subseteq \mathbf{H}} \left[\log_2 \det \left(\mathbf{I}_M + \frac{1}{N \times \sigma^2} \mathbf{H}_{sub} \mathbf{H}_{sub}^H \right) \right], \quad (9)$$

where \mathbf{H}_{sub} denotes the channel matrix from any L -amount AP subset.

Define \mathbf{H}_τ as the matrix obtained by choosing τ columns from \mathbf{H} after τ th selection. Additionally, C_τ denotes the corresponding channel capacity, where $C_\tau = \log_2 \det(\mathbf{I}_M + \bar{\rho} \mathbf{H}_\tau \mathbf{H}_\tau^H)$ and $\tau = 0, 1, \dots, L - 1$. (Note that $C_0 = 0$)

Assuming that in the $(\tau + 1)$ th selection step, the k -th column of matrix \mathbf{H} , denoted as \mathbf{h}_k , will be chosen from the remaining candidate set. The resulting $(\tau + 1) \times M$ submatrix is denoted as $\mathbf{H}_{\tau+1} = [\mathbf{H}_\tau \ \mathbf{h}_k]$.

Accordingly, the channel capacity after τ th selection could be obtained as

$$\begin{aligned}
C_{\tau+1} &= \log_2 \det(\mathbf{I}_M + \bar{\rho} \mathbf{H}_{\tau+1} \mathbf{H}_{\tau+1}^H) \\
&= \log_2 \det(\mathbf{I}_M + \bar{\rho} \mathbf{H}_{\tau} \mathbf{H}_{\tau}^H + \bar{\rho} \mathbf{h}_k \mathbf{h}_k^H) \\
&= C_{\tau} + \log_2 \det(\mathbf{I}_M + \bar{\rho} (\mathbf{I}_M + \bar{\rho} \mathbf{H}_{\tau} \mathbf{H}_{\tau}^H)^{-1} \mathbf{h}_k \mathbf{h}_k^H) \\
&\stackrel{(a)}{=} C_{\tau} + \underbrace{\log_2 (1 + \bar{\rho} \mathbf{h}_k^H \mathbf{G}_{\tau} \mathbf{h}_k)}_{\Delta_{k,\tau}},
\end{aligned} \tag{10}$$

Algorithm 1. The BAB-based AP Selection Algorithm with Selection Size Constraint

```

1: INPUT : original channel matrix  $\mathbf{H}$ , number of APs to be selected  $L$ ,  $\text{SNR}\bar{\rho}$ 
2: OUTPUT : final selected AP index vector  $\bar{\mathbf{s}}$ 
3: Initialization:  $\mathbf{G} = \mathbf{I}_M$ ,  $B = -\infty$ ,  $\tilde{C} = M$ ,  $\tau = 0$ ,  $J = 0$ ,  $\mathbf{s} = \mathbf{0}_L$ ,  $\mathcal{K} = \{1, 2, \dots, N\}$ ,
 $\mathcal{L} = \{0, 1, \dots, L-1\}$ ,  $\Delta_0 = \log_2(1 + \bar{\rho} \mathbf{H}^H \mathbf{H})$ 
4:  $\mathcal{I}_{\tau} = \{\tau + 1, \tau + 2, \dots, (N - L + \tau + 1)\} \quad \forall \tau \in \mathcal{L}$ 
5:  $\mathcal{I}_{\tau, K_{\tau}} = \{K_{\tau} + 1, K_{\tau} + 2, \dots, (N - L + \tau + 1)\} \quad \forall \tau \in \mathcal{L}, K_{\tau} \in \mathcal{I}_{\tau-1}$ 
6:  $v_k = \|\mathbf{h}_k\|^2 \quad \forall k \in \mathcal{K}$ 
7:  $\zeta_m = \max_{k \in \mathcal{I}_m} v_k$ ,  $Z_m = \log_2(1 + \bar{\rho} \zeta_m) \quad \forall m \in \mathcal{K}$ 
8:  $c_k = \tilde{C} + \Delta_k - Z_{\tau} \quad \forall k \in \mathcal{I}_{\tau, K}$ 
9: if  $\tau = L - 1$  then
10:   if  $\max_{m \in \mathcal{I}_{L-1}} c_m > B$  then
11:     update:  $[\mathbf{s}]_L = \arg \max_{m \in \mathcal{I}_{L-1}} c_m$ ,  $B = \max_{m \in \mathcal{I}_{L-1}} c_m$ ,  $\bar{\mathbf{s}} = \mathbf{s}$ 
12:   end if
13: else
14:   sort  $c_k$  in descending order and obtain the ordered index vector  $\mathbf{k}$ .
15:    $\mathbf{G}_{tmp} = \mathbf{G}$ ,  $\mathbf{v}_{tmp, j} = \mathbf{v}_k$ 
16:   for  $i = 1 : |\mathcal{I}_{\tau, K}|$  do
17:      $K = [\mathbf{k}]_i$ 
18:     if  $c_K > B$  then
19:        $K = K + 1 : N$ 
20:       update the index vector  $[\mathbf{s}]_{\tau+1} = K$ 
21:        $\mathbf{g} = \frac{1}{\sqrt{\bar{\rho}^{-1} + v_{tmp, K}}} \mathbf{G} \mathbf{h}_K$ ,  $\mathbf{G} = \mathbf{G}_{tmp} - \mathbf{g} \mathbf{g}^H$ ,  $\tilde{C} = c_K$ 
22:       for  $\forall m \in \mathcal{K}$ :
23:          $\xi_m = \mathbf{h}_m^H \mathbf{g}$ ,  $v_m = v_{tmp, m} - |\xi_m|^2$ ,  $\Delta_m = \log_2(1 + \bar{\rho} v_m)$ 
24:          $\tau = \tau + 1$ , return to line 8
25:       else
26:         break this loop
27:       end if
28:     end for
29:   end if

```

where $\bar{\rho} = \frac{1}{N \times \sigma^2}$ represents the Signal-to-Noise Ratio(SNR), Step (a) is established using Sylvester's determinant identity and $G_{\tau} = (\mathbf{I}_M + \bar{\rho} \mathbf{H}_{\tau} \mathbf{H}_{\tau}^H)^{-1}$. It is

obvious that G_τ is positive definite. As a result, the incremental value $\Delta_{k,\tau}$ presented in Eq. (10) is strictly positive when $\mathbf{h}_k \neq 0$, which implies that the channel capacity C_τ monotonically increases as the number of iteration τ enlarges.

Nevertheless, for efficient pruning, the BAB algorithm is only suitable for the monotonically decreasing functions with the determined maximum or the monotonically increasing functions with the determined minimum. Hence, to derive the maximum channel capacity, we have to reorganize a monotonically-decreasing objective function that accommodates the BAB algorithm, since C_τ in Eq. (10) has been proved to be monotonically increasing. Similar to [16], let

$$\tilde{C}_\tau = C_\tau - \sum_{m=0}^{\tau-1} Z_m, \quad (11)$$

where $Z_m = \log_2(1 + \bar{\rho}\zeta_m^2)$ and $\zeta_m = \max_{k \in \mathcal{I}_m} \|\mathbf{h}_k\|_F$. The index set \mathcal{I}_m comprises all the AP indices to be chosen in the m th selection step. The equation in Eq. (11) has a key property presented as follows:

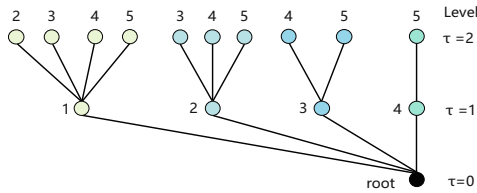


Fig. 2. Example of BAB algorithm: selecting 2 out of 5 APs.

Lemma 1. *The object function \tilde{C}_τ in Eq. (11) monotonically decreases with τ .*

Proof. See Appendix A.

Based on the property mentioned in Lemma 1, since the offset $\sum_{m=0}^{\tau-1} Z_m$ is solely determined by the channel realization and independent of the selected AP subset, the optimal solution achieved by employing the BAB algorithm for the new objective function is equivalent to the optimal solution for the original objective function. Therefore, we propose the algorithm to derive the maximum channel capacity in the user-centric cell-free massive MIMO networks with the L -amount optional APs constraint, as presented in Algorithm 1. Here we use $\mathcal{I}_{\tau,K_\tau}$ to represent the set of child nodes in the $(\tau + 1)$ th layer derived from the parent node K_τ in the τ th layer. The candidate set, encompassing all candidates in the $(\tau + 1)$ th level, is denoted as $\mathcal{I}_\tau = \bigcup_{K_\tau \in \mathcal{I}_{\tau-1}} \mathcal{I}_{\tau,K_\tau}$.

Figure 2 demonstrates the fundamental searching and pruning procedure in the BAB algorithm. By constructing a L -layer multi-branch search tree, we enumerate all the possible L -amount APs selection schemes. During the search operation, we maintain a global variable B (e. g., $-\infty$) and compare it with each

tree-node's value, which can be calculated by Eq. (11). If any of the tree node's value is lower than B , according to Lemma 1, it is evident that the values of all child nodes of that node will also be less than B and therefore subsequent computations at that node can be skipped or "pruned". It should be noted that the variable B is updated only at the leaf nodes at which their values are greater than B and have no child nodes. By iteratively performing the above steps, the optimal solution of the objective function, denoted as \bar{s} , can be obtained upon traversing the entire tree.

Table 1. Simulation parameters

Parameters	Value
UE's antennas M	4
Total APs N	18
APs to be selected L	4
Side length $R(m)$	1500
Path loss α	1
Shadow fading σ_{dB}	1
Simulation times T	2000

4 Simulation Results

In this section, we present simulation results to illustrate the performance of the BAB-based AP Selection Algorithm in user-centric cell-free massive MIMO networks. Specifically, we consider a cell-free networking where one user with M antennas and N single-antenna APs are randomly distributed within a square of side length R . We perform our algorithm to select L APs out of N available ones to serve the user. The detailed parameters of simulations are shown in Table 1.

We compare the proposed algorithm with the optimal algorithm (i.e., exhaustive search) and the other two strategies: Su's algorithm [19] and Jung's algorithm [20]. Su's algorithm calculates the Euclidean norms of the channel matrix and selects the first L APs based on the magnitudes of their corresponding norms, arranged in descending order from largest to smallest. Jung's algorithm, on the other hand, simplifies Eq. (8) under high SNR conditions and derives a new selection criterion as follows: During the initial step, we choose the column of the channel matrix with the highest power. In the n th step ($n \geq 2$), the column that produces the maximum product of the channel gain and the sum of the squared uncorrelated values with the previously selected columns is selected.

Figure 3 presents the correlation between SNR and channel capacity when the AP locations are fixed and the user is randomly distributed. It can be founded that at low SNR levels, the performance differences among all algorithms are marginal. However, as the SNR increases, the distinction between the optimal

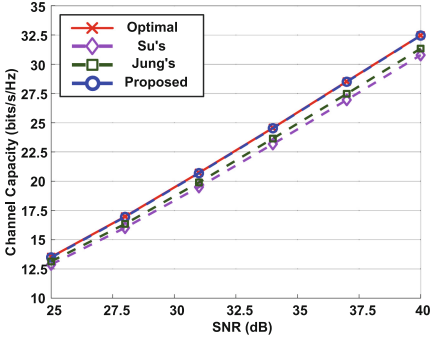


Fig. 3. Channel capacity obtained by different algorithms versus SNR.

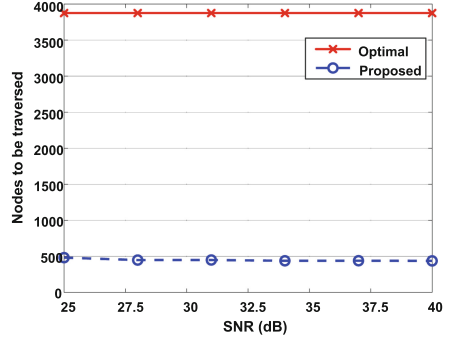


Fig. 4. Nodes to be traversed by exhaustive search and proposed algorithm versus SNR.

Table 2. Complexity comparison

Algorithms	Order of complexity
Optimal	C_N^L
Su's	$O(N)$
Jung's	$O(M \cdot N \cdot L)$
Proposed	$O(M \cdot N \cdot N_{node})$

algorithm and another two algorithms (Su's and Jung's) gradually widens. Simultaneously, the gap between Jung's and Su's algorithms also increases. In contrast, our proposed algorithm (depicted by the blue dotted line with circles) consistently aligns with the optimal curve, demonstrating its ability to achieve a similar optimal performance as exhaustive search.

Table 2 shows the complexity comparison of the above four algorithms, where N_{node} denotes the number of nodes visited during the tree search, depending on the channel realizations. Since N_{node} is usually larger than L , the complexity of our proposed algorithm is slightly higher. Thus, although our algorithm outperforms two baseline algorithms, it sacrifices some complexity.

Figure 4 illustrates the computational complexity of both the exhaustive search and our proposed algorithm by comparing the number of nodes to be traversed. It is evident from the figure that although both algorithms can find the optimal solution, our algorithm traverses only approximately twelve percent of the nodes compared to the exhaustive algorithm, indicating a reduction of more than eighty percent in computational complexity.

Figure 5 demonstrates the channel capacity achieved by exhaustive search and our proposed algorithm, and the gap between the two approaches when the AP locations are fixed and the user is positioned at various locations within the area. Each bulge in the surface map indicates a high likelihood of the existence of

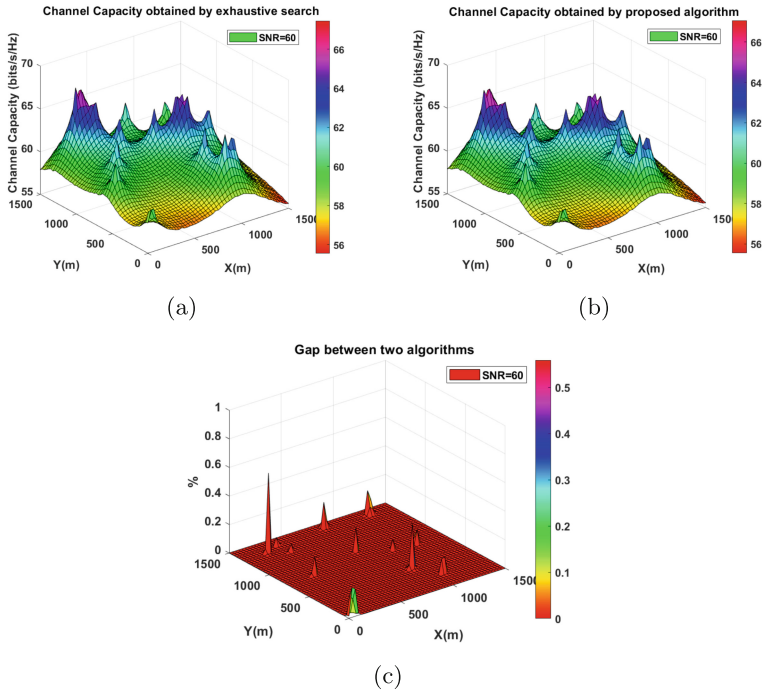


Fig. 5. Channel capacity achieved by (a) exhaustive search, (b) proposed algorithm, and (c) the performance gap between the proposed algorithm and exhaustive search. $M = 4$, $N = 18$, $L = 3$, $R = 1500$ m, $\alpha = 1$, $\sigma_{dB} = 1$ and SNR = 60 dB.

an individual AP. It can be observed from Fig. 5(c) that the proposed algorithm can effectively attain a similar optimal solution at almost every location within the region.

5 Conclusion

This paper focuses on AP selection problems in user-centric cell-free massive MIMO, where only a portion of the APs are dedicated to serving the user. To optimize the channel capacity while adhering to a selection size constraint, we formulate the AP selection problem as a mathematical matrix subset selection problem and propose a Branch-and-Bound (BAB)-based algorithm. Through constructing a multi-branch search tree and fast pruning, our proposed algorithm can efficiently find the optimal AP subset quickly. Simulation results demonstrate that the algorithm we propose is much closer to the optimal solution than the two baselines. Additionally, our algorithm achieves a noteworthy reduction in complexity. Looking forward, we are interested in exploring multi-user scenarios that consider Interference-plus-Noise Ratio (SINR), which aligns more closely with practical wireless communication systems.

Funding. The work was supported in part by National Key R&D Program of China 2022YFB2902004, in part by Guangdong Basic and Applied Basic Research Foundation under Grant 2024A1515012015, in part by The Shenzhen Science and Technology Program (No. RCBS20210706092408010), in part by National Natural Science Foundation of China under Grant 62001524, and in part by the Fundamental Research Funds for the Central Universities, Sun Yat-sen University, under Grant 24pnpy20.

A Proof of Lemma 1

Based on Eqs. (10) and (11), the recursive formulation of \tilde{C}_n is

$$\tilde{C}_{\tau+1} = \tilde{C}_\tau + \Delta_{k,\tau} - Z_\tau, \tau = 0, 1, \dots, L-1. \quad (12)$$

It is evident that if $\Delta_{k,\tau} \leq Z_\tau$ holds for any τ , the function $\tilde{C}_{\tau+1}$ monotonically decreases. Before that, we get $\mathbf{G}_{\tau+1}$ from Eq. (10) as:

$$\begin{aligned} \mathbf{G}_{\tau+1} &= (\mathbf{I}_M + \bar{\rho} \mathbf{H}_{\tau+1}^H \mathbf{H}_{\tau+1})^{-1} \\ &= (\mathbf{I}_M + \bar{\rho} \mathbf{H}_\tau^H \mathbf{H}_\tau + \bar{\rho} \mathbf{h}_{J_\tau} \mathbf{h}_{J_\tau}^H)^{-1} \\ &= \mathbf{G}_\tau - \mathbf{g}_{\tau+1} \mathbf{g}_{\tau+1}^H, \tau = 0, 1, \dots, L-1, \end{aligned} \quad (13)$$

where $\mathbf{g}_{\tau+1} = \frac{\mathbf{G}_\tau \mathbf{h}_{K_\tau}}{\sqrt{\bar{\rho}^{-1} + \mathbf{h}_{K_\tau}^H \mathbf{G}_\tau \mathbf{h}_{K_\tau}}}$, K_τ is the AP index found in the τ th step. Thus, we have

$$\mathbf{G}_\tau = \begin{cases} \mathbf{I}_M, & \tau = 0, \\ \mathbf{I}_M - \sum_{m=1}^{\tau} \mathbf{g}_m \mathbf{g}_m^H, & \tau = 1, 2, \dots, L-1. \end{cases} \quad (14)$$

Next we proceed to prove that $\Delta_{k,\tau} \leq Z_n$ holds for any τ , which could be discussed by the following parts:

1. For $\tau = 0$, we have

$$\begin{aligned} \Delta_{k,0} &= \log_2 (1 + \bar{\rho} \mathbf{h}_k^H \mathbf{h}_k) \\ &\stackrel{(b)}{\leq} \log_2 (1 + \bar{\rho} \zeta_0^2) = Z_0, \end{aligned} \quad (15)$$

where the inequality (b) holds in the 0th selection step for candidate AP index $k \in \mathcal{I}_0$.

2. For $\tau = 1, 2, \dots, L-1$. We define $\bar{\mathbf{G}}_\tau = \sum_{m=1}^{\tau} \mathbf{g}_m \mathbf{g}_m^H$. As the Gram matrix $\mathbf{g}_m \mathbf{g}_m^H$ is positive semi-definite, the summation of positive semi-definite matrices, denoted as $\bar{\mathbf{G}}_\tau$, also constitutes a positive semi-definite matrix. Then it can be inferred that:

$$\mathbf{h}_k^H \mathbf{G}_\tau \mathbf{h}_k - \mathbf{h}_k^H \mathbf{h}_k = -\mathbf{h}_k^H \bar{\mathbf{G}}_\tau \mathbf{h}_k \leq 0. \quad (16)$$

Thus, we have

$$\begin{aligned} \Delta_{k,\tau} &= \log_2 (1 + \bar{\rho} \mathbf{h}_k^H \mathbf{G}_\tau \mathbf{h}_k) \\ &\leq \log_2 (1 + \bar{\rho} \mathbf{h}_k^H \mathbf{h}_k) \\ &\stackrel{(c)}{\leq} \log_2 (1 + \bar{\rho} \zeta_\tau^2) = Z_\tau, \end{aligned} \quad (17)$$

where the inequality (c) holds in the τ th selection step for candidate AP index $k \in \mathcal{I}_\tau$.

In conclusion, the new object function \tilde{C}_τ in Eq. (11) monotonically decreases with τ .

References

1. Wang, J., Dai, L., Yang, L., Bai, B.: Clustered cell-free networking: a graph partitioning approach. *IEEE Trans. Wirel. Commun.* **22**(8), 5349–5364 (2023)
2. Du, M., Sun, X., Zhang, Y., Wang, J., Liu, P.: Joint cooperation clustering and downlink power control for cell-free massive MIMO with deep reinforcement learning. In: *Proceedings of IEEE ICCT* (2023)
3. Zhang, H., Su, R., Zhu, Y., Long, K., Karagiannidis, G.K.: User-centric cell-free massive MIMO system for indoor industrial networks. *IEEE Trans. Commun.* **70**(11), 7644–7655 (2022)
4. Wei, C., et al.: User-centric access point selection in cell-free massive MIMO systems: a game-theoretic approach. *IEEE Commun. Lett.* **26**(9), 2225–2229 (2022)
5. Buzzi, S., D’Andrea, C.: Cell-free massive MIMO: user-centric approach. *IEEE Wirel. Commun. Lett.* **6**(6), 706–709 (2017)
6. Ammar, H.A., Adev, R., Shahbazpanahi, S., Boudreau, G., Srinivas, K.V.: User-centric cell-free massive MIMO networks: a survey of opportunities, challenges and solutions. *IEEE Commun. Surv. Tutor.* **24**(1), 611–652 (2021)
7. Ngo, H.Q., Tran, L.-N., Duong, T.Q., Matthaiou, M., Larsson, E.G.: On the total energy efficiency of cell-free massive MIMO. *IEEE Trans. Green Commun. Netw.* **2**(1), 25–39 (2018)
8. Dai, L.: An uplink capacity analysis of the distributed antenna system (DAS): from cellular DAS to DAS with virtual cells. *IEEE Trans. Wirel. Commun.* **13**(5), 2717–2731 (2014)
9. Wang, J., Dai, L.: Downlink rate analysis for virtual-cell based large-scale distributed antenna systems. *IEEE Trans. Wirel. Commun.* **15**(3), 1998–2011 (2016)
10. Mai, T.C., Ngo, H.Q., Egan, M., Duong, T.Q.: Pilot power control for cell-free massive MIMO. *IEEE Trans. Veh. Technol.* **67**(11), 11264–11268 (2018)
11. Attarifar, M., Abbasfar, A., Lozano, A.: Subset MMSE receivers for cell-free networks. *IEEE Trans. Wirel. Commun.* **19**(6), 4183–4194 (2020)
12. Interdonato, G., Karlsson, M., Björnson, E., Larsson, E.G.: Local partial zero-forcing precoding for cell-free massive MIMO. *IEEE Trans. Wirel. Commun.* **19**(7), 4758–4774 (2020)
13. Liu, H., Zhang, J., Jin, S., Ai, B.: Graph coloring based pilot assignment for cell-free massive MIMO systems. *IEEE Trans. Veh. Technol.* **69**(8), 9180–9184 (2020)
14. Buzzi, S., D’Andrea, C., Zappone, A., D’Elia, C.: User-centric 5G cellular networks: resource allocation and comparison with the cell-free massive MIMO approach. *IEEE Trans. Wirel. Commun.* **19**(2), 1250–1264 (2020)

15. Wei, C., et al.: User-centric access point selection in cell-free massive MIMO systems: a game-theoretic approach. *IEEE Commun. Lett.* **26**(9), 2225–2229 (2022)
16. Gao, Y., Vinck, H., Kaiser, T.: Massive MIMO antenna selection: switching architectures, capacity bounds, and optimal antenna selection algorithms. *IEEE Trans. Signal Process.* **66**(5), 1346–1360 (2018)
17. Gong, Y., Wang, X.: Channel capacity analysis and simulations of distributed MIMO system. In: *Proceedings of IEEE WiCOM* (2009)
18. Gao, Y., Khaliel, M., Zheng, F., Kaiser, T.: Rotman lens based hybrid analog-digital beamforming in massive MIMO systems: array architectures, beam selection algorithms and experiments. *IEEE Trans. Veh. Technol.* **66**(10), 9134–9148 (2017)
19. Su, Y., Feng, G.: A novel fast antenna selection algorithm in distributed MIMO systems. In: *Proceedings of IEEE ICCT* (2010)
20. Jung, S.-Y., Kim, B.W.: Near-optimal low-complexity antenna selection scheme for energy-efficient correlated distributed MIMO systems. *Int. J. Electron. Commun.* **69**(7), 1039–1046 (2015)